nature microbiology

SUPPLEMENTARY INFORMATION

DOI: 10.1038/s41564-017-0014-5

In the format provided by the authors and unedited.

Interspecies quorum sensing in co-infections can manipulate trypanosome transmission potential

Eleanor Silvester, Julie Young, Alasdair Ivens and Keith R. Matthews*

Centre for Immunity, Infection and Evolution, Institute for Immunology and Infection Research, School of Biological Sciences, University of Edinburgh, Edinburgh, EH9 3FL, UK. *e-mail: keith.matthews@ed.ac.uk

Interspecies quorum-sensing in co-infections can manipulate trypanosome transmission potential

Eleanor Silvester, Julie Young, Alasdair Ivens, and Keith R. Matthews

Supplementary data

Predicted gene function	*T. brucei* ID	*T. congolense* ID	% identity	% similarity	Reciprocal BLAST?
Protein phosphatase	Tb927.4.3620	TcIL3000.11.8600	58	78	
Protein phosphatase	Tb927.4.3640	TcIL3000.11.8600	57	78	
Protein phosphatase	Tb927.4.3630	TcIL3000.11.8600	57	78	
Protein Kinase	Tb927.10.5940	TcIL3000.10.4970	89	95	●
Protein Kinase	Tb927.10.5930	TcIL3000.10.4970	90	95	
Protein Kinase	Tb927.10.5950	TcIL3000.10.4970	88	93	
Protein Kinase	Tb927.2.2720	TcIL3000.0.44450	39	54	●
Protein Kinase	Tb927.10.15020	TcIL3000.10.12870	49	63	●
Hypothetical Protein (Hyp 1)	Tb927.11.6600	TcIL3000.11.7200	46	62	●
Hypothetical Protein (Hyp 2)	Tb927.9.4080	TcIL3000.0.19510	45	58	●
RNA-binding protein	Tb927.10.12100	TcIL3000.10.10320	73	81	
Adenylosuccinate synthetase (Purine pathway)	Tb927.11.3650	TcIL3000.11.3610	86	93	●
Adenylosuccinate Lyase (Purine pathway)	Tb927.9.7550	TcIL3000.0.18960	82	91	●
GMP synthase	Tb927.7.2100	TcIL3000.0.55050	77	87	●
ubiquitin activating enzyme, putative	Tb927.2.4020	TcIL3000.2.550	54	70	●
serine/threonine protein kinase, putative	Tb927.3.4560	TcIL3000.10.4460	51	69	
hypothetical protein, conserved (Hyp 3)	Tb927.4.670	TcIL3000.4.290	59	74	●
hypothetical protein (Hyp 4)	Tb927.4.3650	TcIL3000.10.810	25	44	
adenosine kinase, putative	Tb927.6.2300	TcIL3000.6.1860	72	86	
adenosine kinase, putative	Tb927.6.2360	TcIL3000.6.1860	73	86	●
kinetoplastid-specific dual specificity phosphatase, putative	Tb927.7.7160	TcIL3000.0.52520	41	52	●
hypothetical protein, conserved (Hyp 6)	Tb927.9.13530	TcIL3000.9.5770	48	66	●
inosine-5'-monophosphate dehydrogenase	Tb927.10.16120	TcIL3000.5.1940	37	55	
phosphatase and tensin homologue, putative	Tb927.11.290	TcIL3000.11.210	67	80	●
protein kinase A regulatory subunit	Tb927.11.4610	TcIL3000.0.15340	76	88	●
transcription silencer (ISWI)	Tb927.2.1810	TcIL3000_2_50	62	76	●
Phosphoglycerate mutase	Tb927.5.3580	TcIL3000_0_40660	79	90	●
Hypothetical protein (Hyp 5)	Tb927.8.2860	TcIL3000_0_41460	40	56	●
Hypothetical protein, conserved (Hyp 8)	Tb927.11.300	TcIL3000.11.220	53	65	●
DNA repair protein, putative (Hyp 9)	Tb927.11.750	TcIL3000_0_15260	72	85	●
Product: protein phosphatase 2C, putative	Tb927.11.760	TcIL3000_0_15250	83	90	●
Hypothetical protein, conserved (Hyp 10)	Tb927.11.1640	TcIL3000.11.1420	42	60	●
Hypothetical protein, conserved (Hyp 11)	Tb927.11.2250	TcIL3000.11.2000	45	67	●
Hypothetical protein, conserved (Hyp 13)	Tb927.11.11470	TcIL3000_0_22050	66	75	●
Trichohyalin, putative	Tb927.11.11480	TcIL3000_0_28560	63	80	●

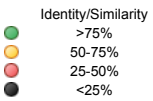

Supplementary Table 1

T. congolense encodes predicted orthologues of components of the T. brucei stumpy formation pathway.

T. brucei QS-signalling molecules were analysed by BLASTP at TritrypDB (http://tritrypdb.org/tritrypdb/). *T. congolense* was selected as the target organism and default parameters were used. The top *T. congolense* hit is reported alongside the respective % identity and % similarity of the amino acid sequences. A green dot in the final column indicates that the top *T. congolense* hit returned the original *T. brucei* protein when reciprocal BLAST was performed.

Hypothetical Protein 2 (Tb927.9.4080)	
Function or annotation	Hypothetical, conserved (HYP2)
Annotation in TritrypDB	Component of the stumpy induction factor (SIF) signalling pathway (IMP, PMID:24336212)[1] Fragments of this protein increase translation or mRNA stability when tethered to a reporter mRNA (PMID:24945722)[2] Interacts with MKT1 (PMID:24470144; IPI)[3]
RITSeq Phenotype[4]	Loss-of-fitness in differentiation from bloodstream to procyclic forms
SIF resistance[1]	RNAi targeting HYP2 results in resistance to SIF and therefore reduced stumpy formation *in vivo*
Predicted domains[5]	Prokaryotic dksA C4-type zinc finger signature and profile (InterPro IPR000962, PROSITE PS51128); P-loop containing nucleoside triphosphate hydrolases (InterPro IPR027417, Superfamily SSF52540, Gene3D G3DSA:3.40.50.300); DNA ligase/ mRNA capping enzyme (Superfamily SSF56091, Gene3D G3DSA:3.30.470.30)
Eukaryotic linear motifs[6]	Phosphorylation sites favoured by PKA-type AGC kinase (MOD_PKA_1 and _2), NEK2(MOD_NEK2_1 and _2) or CDK (MOD_CDK_1); PP1 catalytic subunit interaction motif (DOC_PP1_RVXF_1), docking motif that assists in regulating specific interactions with the MAPK cascade (DOC_MAPK_1), motif for eIF4E binding (LIG_eIF4E_1), Retinoblastoma protein interaction domain (LIG_Rb_LxCxE_1), BRCA1 interaction domain (LIG_BRCT_BRCA1_1), potential interaction with TNFR signalling pathway (LIG_TRAF2_1)
mRNA expression profile[7]	Slender – 62.6, Intermediate – 65.0, Stumpy - 59.6
Protein expression PCF/BSF[8]	1.1406
Phospho site[9]	S258

Much of this information is available in the Supplementary tables of Mony et al Nature **2014** 505 (7485): p. 681-5

Source data

1. Mony et al Nature **2014** 505 (7485): p. 681-5
2. Erben et al PLoS Pathogens **2014** 10: e1004178
3. Singh et al Nucleic acids research **2014** 42: 4652-4668
4. Alsford et al Genome Research **2011** 21: 915-924
5. Finn et al Nucleic acids Research **2017** 45: D190-D199
6. Dinkel et al Nucleic acids Research **2012** 40: D242-251
7. Capewell et al PLoS One **2013** 8 (6): e67069
8. Urbaniak et al PLoS One **2012** 7 (5): e36619
9. Urbaniak et al J. Proteome Res. **2013** 12 (5): pp 2233-2244

Supplementary Table 2

Characteristics of *Tb*HYP2 based on its sequence, motifs, expression and functional information available in the sources indicated.

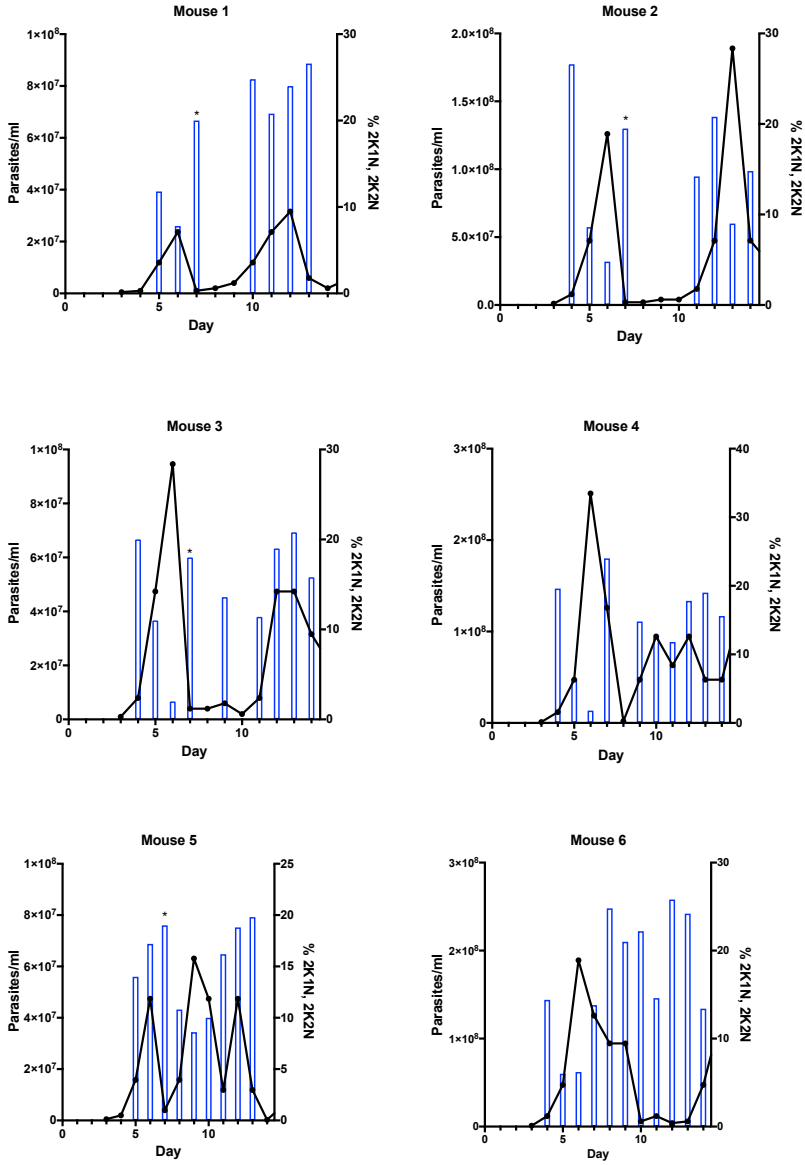

Supplementary Figure 1

Parasitaemia and cell cycle analysis for six T. congolense infections from days 3-14 post-infection.

For each infection a black line represents the parasitaemia, and blue bars represent the percentage of proliferating cells (2K1N – G2-phase cells, 2K2N – post-mitotic cells). The percentage of proliferating cells was calculated by analysing the kinetoplast and nuclear configuration of 500 cells (except for bars marked with an asterisk for which 200 cells were analysed due to the low parasitaemia at these timepoints). When parasitaemia exceeded approximately $8x10^7$/ml a reduction in proliferating cells was observed.

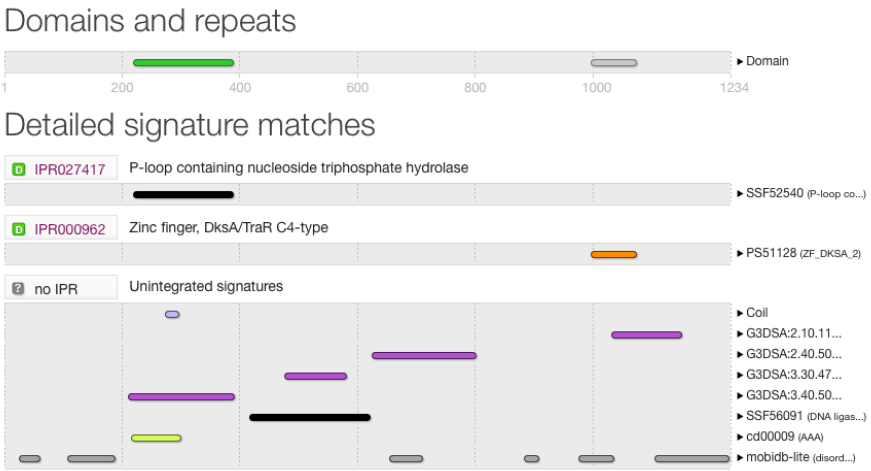

Supplementary Figure 2

Characteristics of *Tb*HYP2 showing the location of predicted domains detected within the protein. Screenshot taken from an InterPro search with Tb927.9.4080 amino acid sequence (https://www.ebi.ac.uk/interpro/, Finn et al Nucleic acids Research **2017** 45: D190-D199)

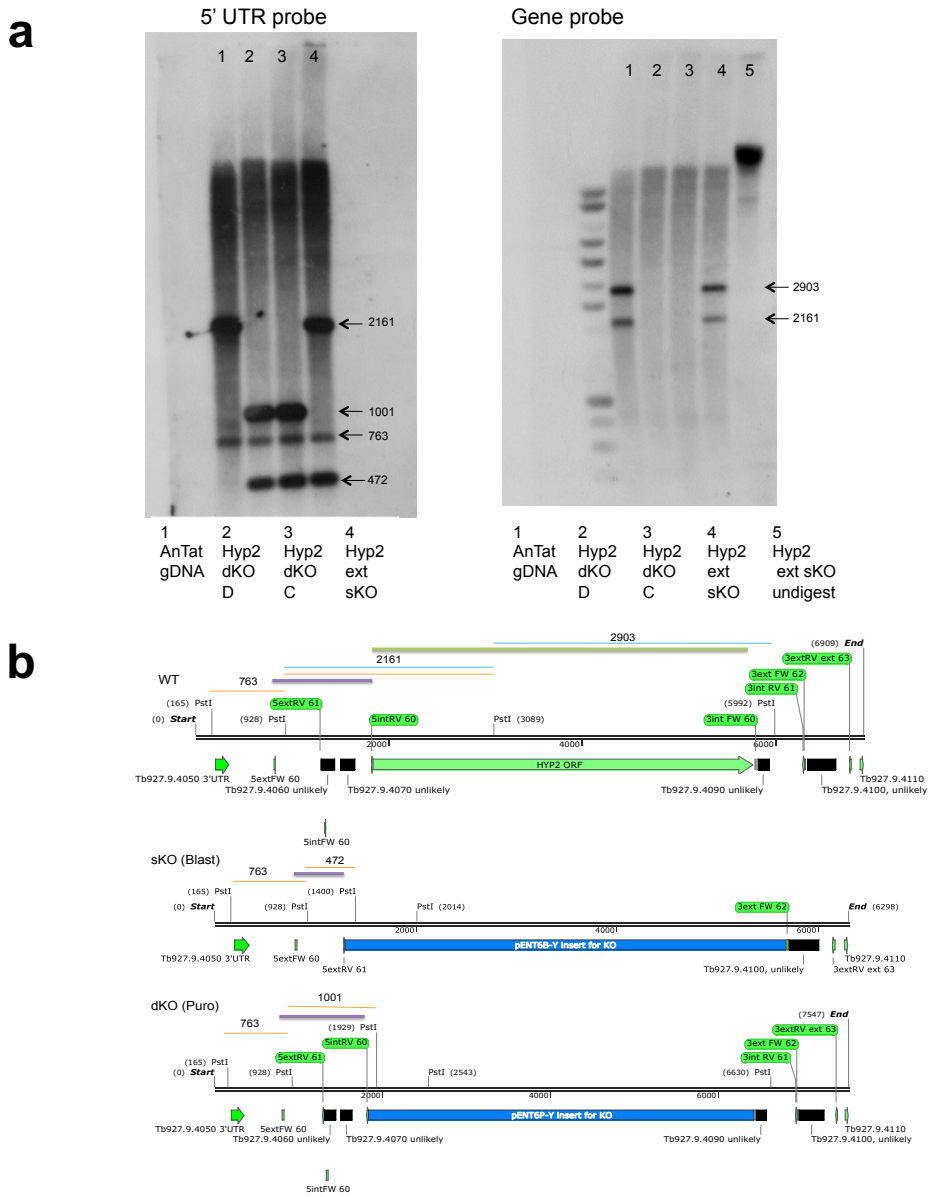

Supplementary Figure 3

Generation of a TbHYP2 (Tb927.9.4080) null mutant in a T. brucei AnTat 1.1 90.13 background.

a) Generation of *TbHYP2* null mutants by sequential allelic replacement was confirmed by the restriction digest of genomic DNA from two clonal cell lines with PstI followed by Southern blotting. The use of probes targeted to either the 5'UTR or coding region of *TbHYP2* revealed a characteristic digest pattern that matched expectation confirming successful generation of two *Tb*HYP2 null mutants (C and D). *TbHYP2* null mutant clone C was selected for further experimentation.

b) Schematic representation of expected banding patterns for the wild-type (WT) allele, the first allelic replacement (sKO) or the second allelic replacement (dKO). Predicted band sizes obtained with the 5'UTR probe are represented by orange lines, those expected with the gene probe are represented by blue lines. The total region detectable by the gene probe is represented by a thick green line. The total region detectable by the 5'UTR probe is represented by a thick purple line.

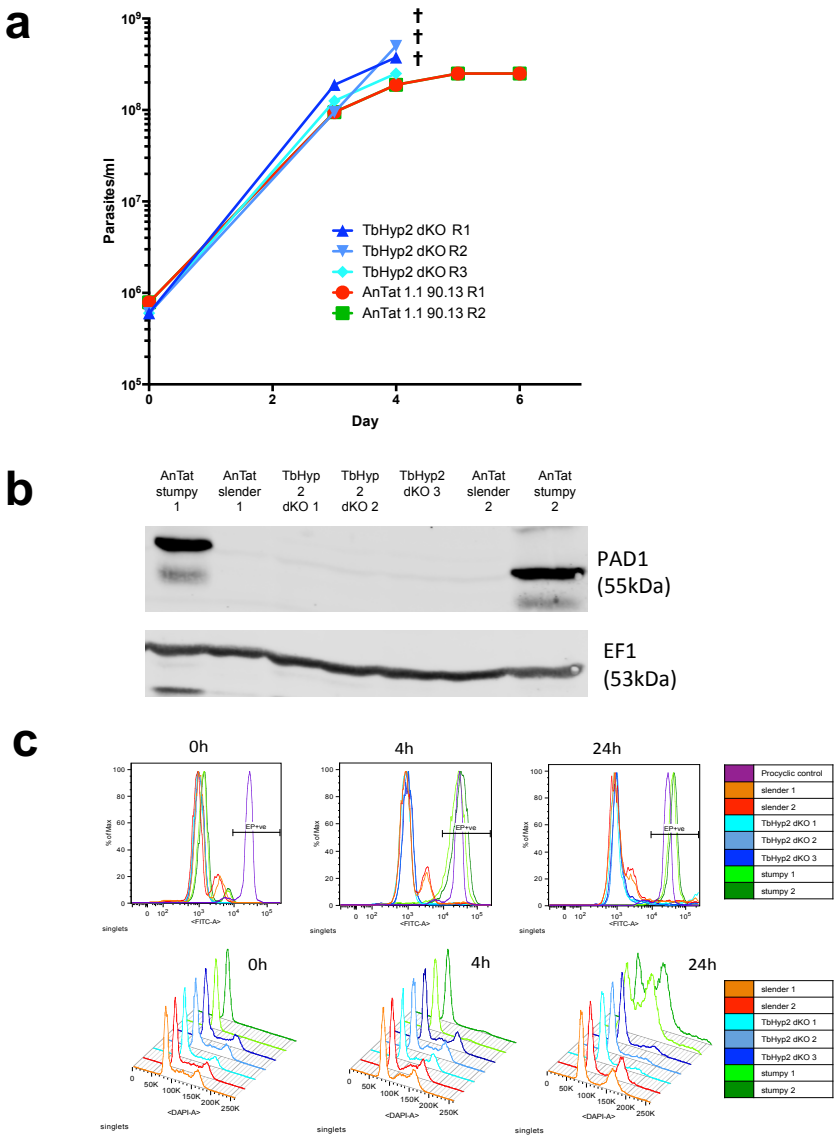

Supplementary Figure 4

Infections with a TbHYP2 null mutant reach high parasitaemia without evidence of growth control or differentiation to stumpy forms.

a) Infections with the *TbHYP2* null mutant (n=3) were monitored alongside infections with the parental *T. brucei* AnTat 1.1 90.13 line (n=2). Infections were terminated when ascending parasitaemias were predicted to become lethal within 12h (crosses).
b) *TbHYP2* null mutant cells did not express the stumpy marker PAD1 despite high parasitaemia as visualised by western blot. EF1 was used as a loading control.
c) *TbHYP2* null mutant cells showed reduced capacity to differentiate to procyclic forms following induction with 6mM cis-aconitate, as determined by EP procyclin expression at 4h and 24h after induction. Additionally, *Tb*HYP2 null mutant cells showed reduced proliferation after 24h of induction with cis-aconitate, compared to both slender (3 days post infection) and stumpy (6 days post infection) control parasites. The EP procyclin expression and cell cycle data were obtained by flow cytometry.

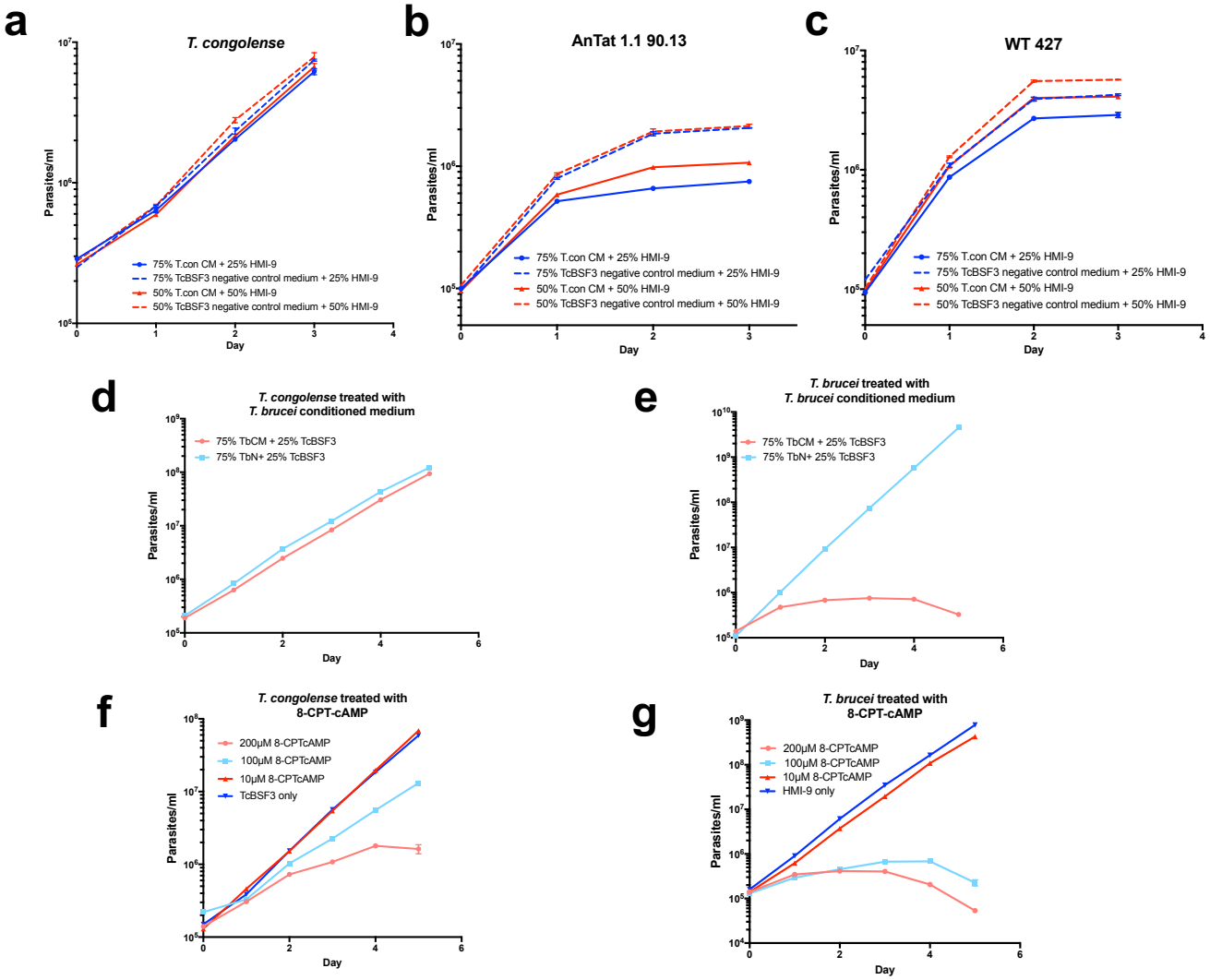

Supplementary Figure 5

a-c) The effect of T. congolense conditioned medium on T. brucei pleomorphic and monomorphic cell lines, and T. congolense itself.

d-g) The effect of T. brucei conditioned medium and 8-pCPTcAMP on T. congolense and pleomorphic T. brucei.

a) The effect of *T. congolense* conditioned medium on *T. congolense* IL3000.

b) The effect of *T. congolense* conditioned medium on pleomorphic *T. brucei* EATRO 1125 AnTat1.1 90:13.

c) The effect of *T. congolense* conditioned medium on monomorphic Lister 427 *T. brucei*.

d) The effect of 75% *T. brucei* conditioned medium on *T. congolense* IL3000.

e) The effect of 75% *T. brucei* conditioned medium on *T. brucei* EATRO 1125 AnTat1.1 90:13.

f) The response of *T. congolense* IL3000 to the cell permeable QS-signal mimic 8-pCPTcAMP.

g) The response of *T. brucei* EATRO 1125 AnTat1.1 90:13 to the cell permeable QS-signal mimic 8-pCPTcAMP.

Each data point represents the mean of triplicate wells; error bars represent SEM, and are sometimes obscured by the data point due to the high reproducibility of the assays.

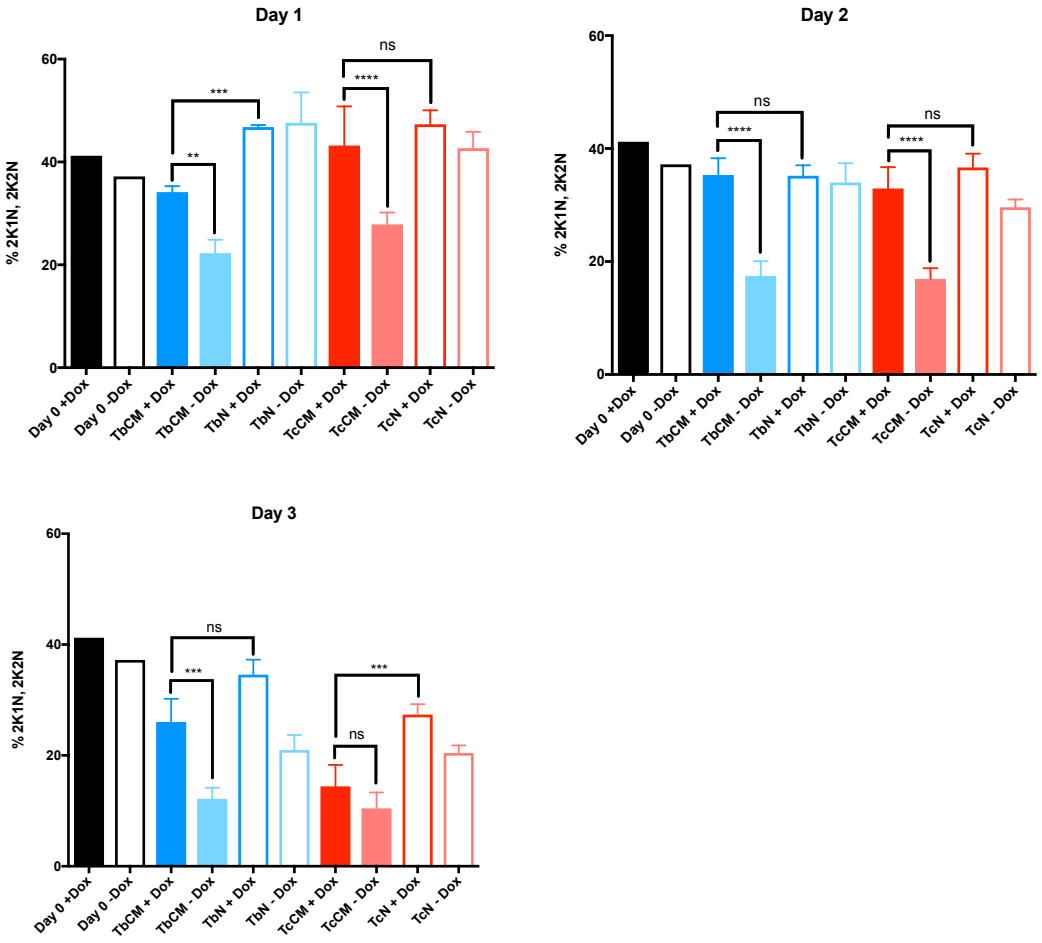

Supplementary Figure 6

Cell cycle status of T. brucei following treatment with T. brucei or T. congolense conditioned medium with (+Dox) or without (-Dox) induction of RNAi targeting TbHYP2

The pleomorphic cell line *T. brucei* AnTat1.1 90:13 CAT-PAD *TbHYP2* RNAi was treated with *Tb*CM or *Tc*CM and cells collected on days 1-3 of the experiment were scored for their kinetoplast and nuclear configuration. Each bar represents the mean and standard deviation of triplicate flasks (250 cells counted for each replicate). There was a reduction in the proportion of proliferating (2K1N, 2K2N) cells following treatment with *Tb*CM or *Tc*CM when RNAi was not induced. The reduction in proliferating cells was muted when *TbHYP2* RNAi had been induced relative to uninduced cells. Comparisons between categories were made using two-way ANOVA followed by Tukey's multiple comparison test (★ $p<0.05$, ★★ $p<0.01$, ★★★ $p<0.001$, ★★★★ $p<0.0001$). The effect of *Tc*CM and *Tb*CM on this cell line was reproducible in two (out of two) independent experiments (one representative experiment is shown).

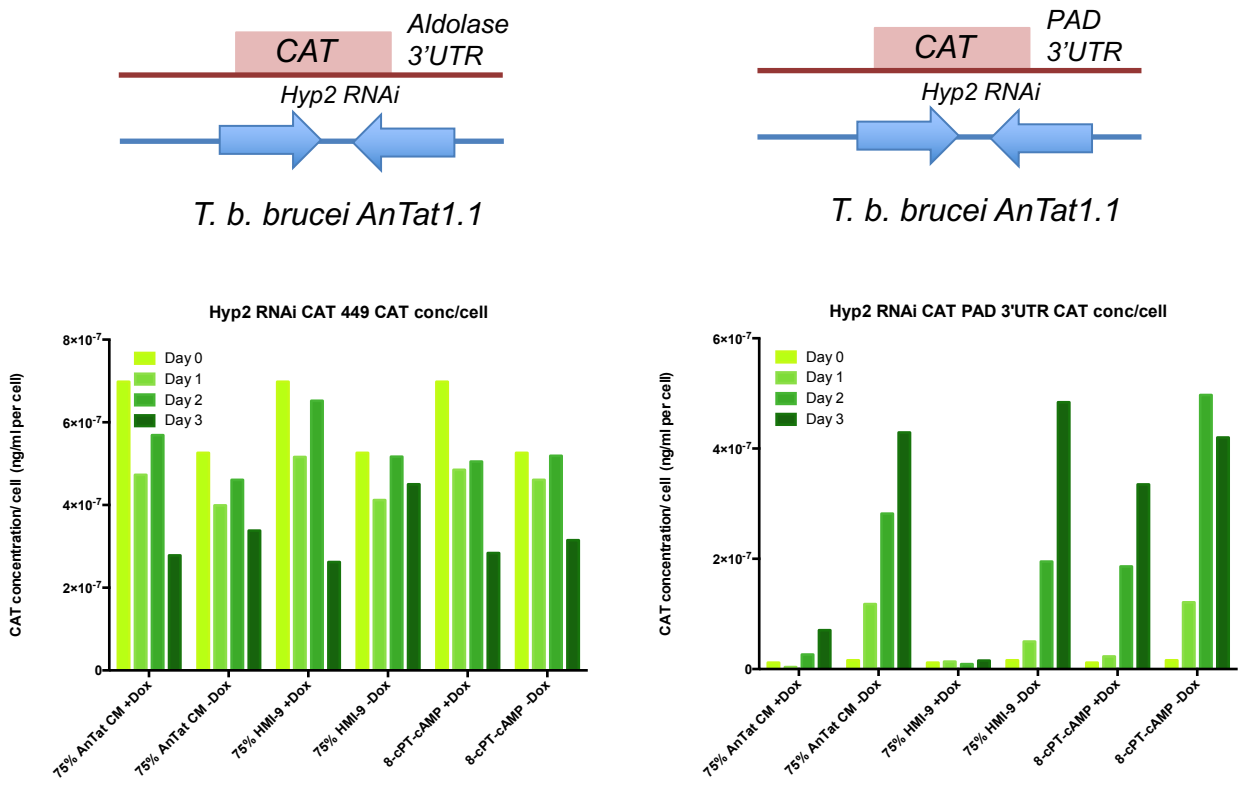

Supplementary Figure 7

The effect of T. brucei conditioned medium and 8-pCPT-cAMP on a pleomorphic reporter line with inducible TbHYP2 RNAi.

A pleomorphic *T. brucei* cell line (EATRO 1125; AnTat 1.1 90.13) capable of doxycycline inducible knock down of *TbHYP2* was transfected with either of two constructs. One construct encoded a CAT reporter with expression under the control of an aldolase 3'UTR. When the cell line with this control construct was treated with conditioned medium or the QS-signal mimic 8-pCPT-cAMP there was no effect on CAT concentration/cell related to RNAi against *TbHYP2*. The second construct encoded a CAT reporter with expression under the control of the *PAD1* 3'UTR. When the cell line with the *CAT PAD* construct was treated with conditioned medium (AnTat CM) or 8-pCPT-cAMP the CAT concentration/cell increased relative to the negative control (75% HMI-9). However, when *TbHYP2* RNAi was induced (+Dox) the CAT concentration/cell did not increase with conditioned medium treatment. For each condition tested n=1.

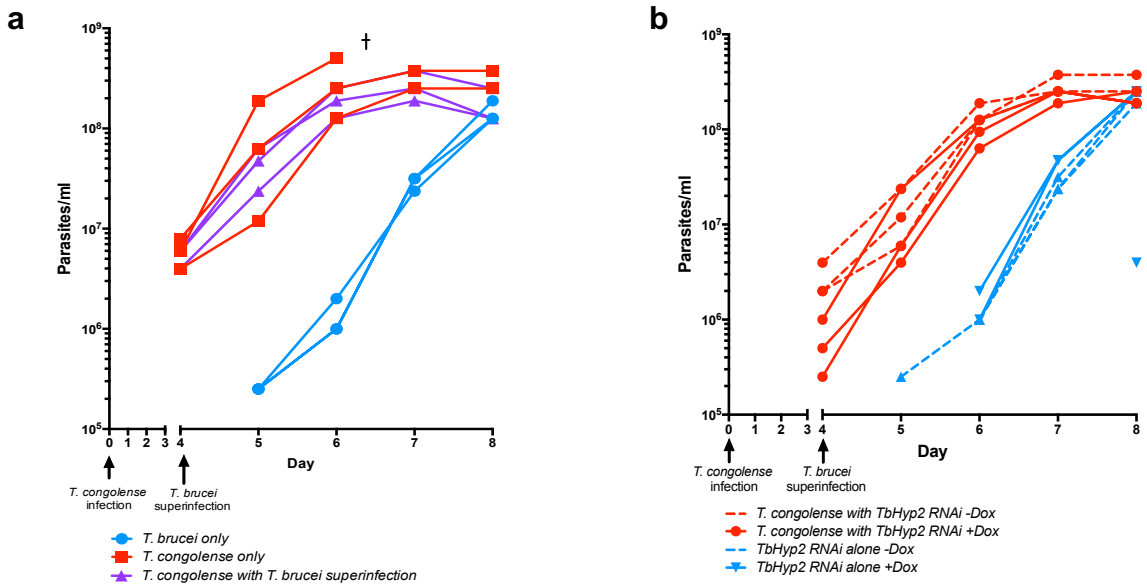

Supplementary Figure 8

Total parasite load in T. congolense/T. brucei co-infections or in single species infections.

a) Superinfections with *T. brucei* AnTat1.1 90:13 PFR-Ty were initiated on day 4 after initiating *T. congolense* infections. Control infections with *T. congolense* only or *T. brucei* only were established in parallel. The total parasitaemia of the co-infections (purple, n=3) followed similar trajectories to the '*T. congolense* only' infections (red, n=3). The '*T. brucei* only' infections (blue, n=3) were in an ascending phase as the *T. congolense* infections were peaking, but reached a similar overall parasitaemia on day 8 of the experiment as the mixed infection.
b) Superinfections with *T. brucei* AnTat1.1 90:13 PFR-Ty1 *TbHYP2* RNAi were initiated on day 4 after initiating *T. congolense* infections. Control infections with *T. brucei* AnTat1.1 90:13 PFR-Ty1 *TbHYP2* RNAi only were established in parallel. *T. brucei* AnTat1.1 90:13 PFR-Ty1 *TbHYP2* RNAi challenge on day 4 was preceded by treatment with sucrose water +/-Dox on day 1. The total parasitaemia for each infection on days 4-8 of the experiment is shown (n=3 for each condition tested). One '*T. brucei* only' infection +Dox infected poorly and was delayed in the appearance of parasites in the blood, relative to other infections.

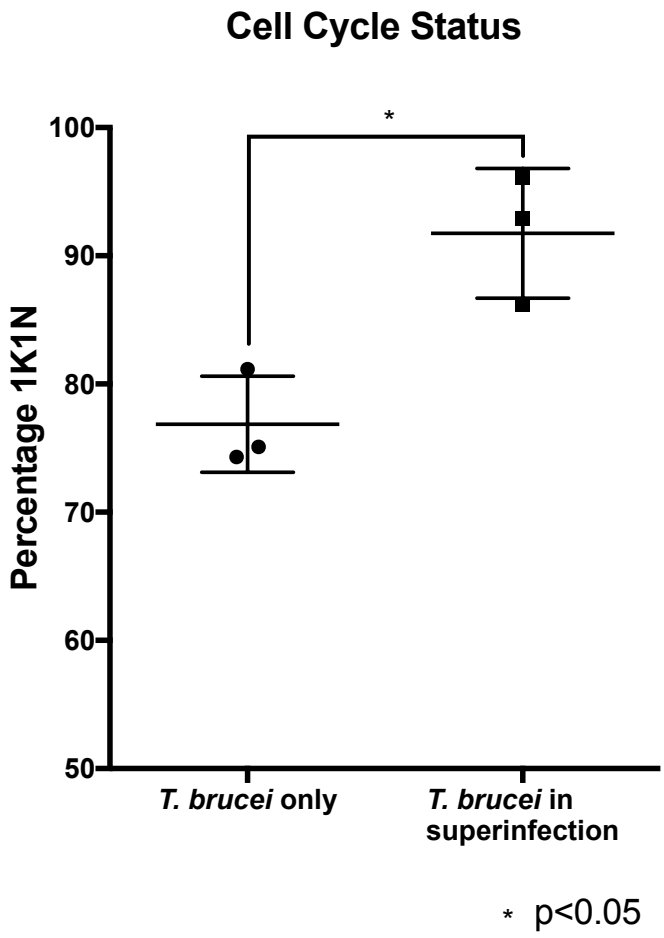

Supplementary Figure 9
Cell cycle status of T. brucei in co-infection with T. congolense or in a single species infection.

T. brucei cells collected on day 8 of the experiment were scored for their kinetoplast and nuclear configuration (>500 cells scored, n=3 for each condition tested). Error bars represent mean ± SD. The lower *T. brucei* parasitaemia in the superinfections was associated with a significantly higher proportion of 1K1N cells compared to that observed in the single species *T. brucei* infections (unpaired t test, ★ $p<0.05$, two-sided).

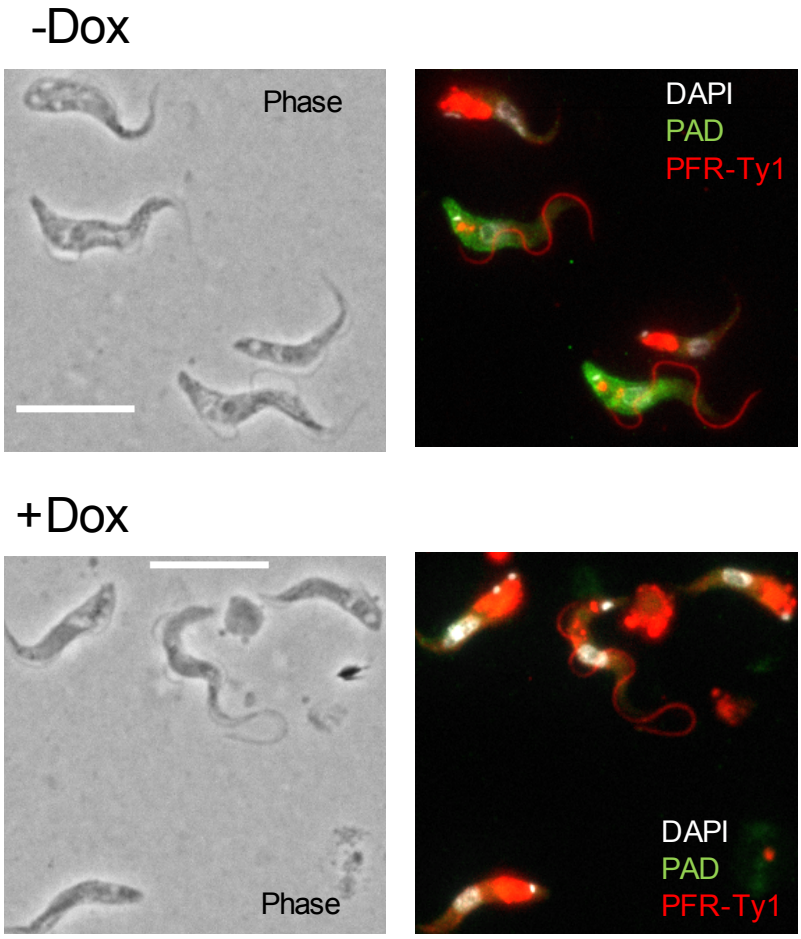

Supplementary Figure 10
Representative images of day 8 superinfection samples with (+Dox) or without (-Dox) induction of RNAi targeting TbHYP2.

An example of PAD1-positive, intermediate/stumpy *T. brucei* cells accompanied by *T. congolense* on day 8 of the co-infection experiment when *TbHYP2* RNAi has not been induced (-Dox), and an example of a PAD1-negative, slender *T. brucei* cell accompanied by *T. congolense* when *TbHYP2* RNAi has been induced (+Dox). PFR-Ty1 (red), PAD1 (green), DAPI (white). Note that *T. congolense* cells show non-specific intracellular staining with the BB2 antibody that detects the Ty1 epitope. Scale bar represents 10μm

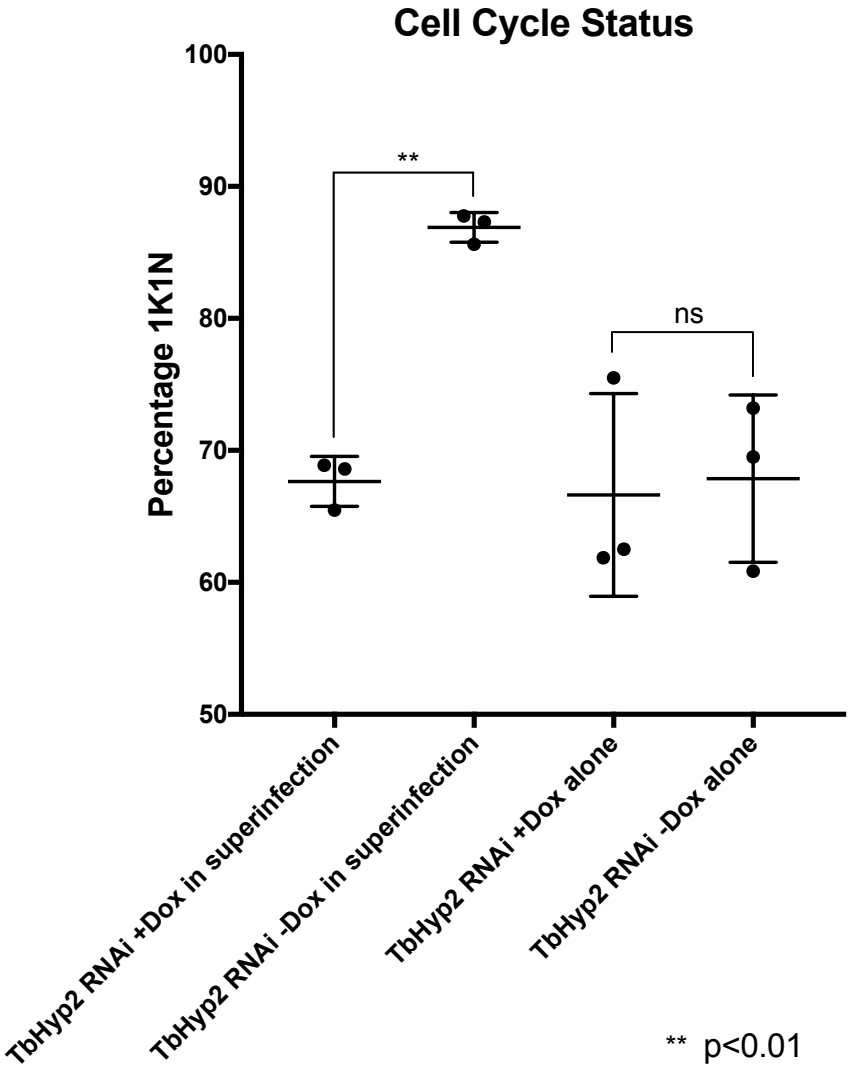

Supplementary Figure 11

Cell cycle status of T. brucei in co-infection with T. congolense or in a single species infection with or without the induction of RNAi targeting TbHYP2.

T. brucei cells collected on day 8 of the experiment were scored for their kinetoplast and nuclear configuration (>500 cells scored, n=3 for each condition tested). Error bars represent mean ± SD. There was a significantly higher proportion of 1K1N *T. brucei* cells when *TbHYP2* RNAi was not induced (-Dox), than when *TbHYP2* RNAi was induced (+Dox) in a co-infection with *T. congolense* (★★ p<0.01, One-way ANOVA with Tukey's multiple comparisons test).

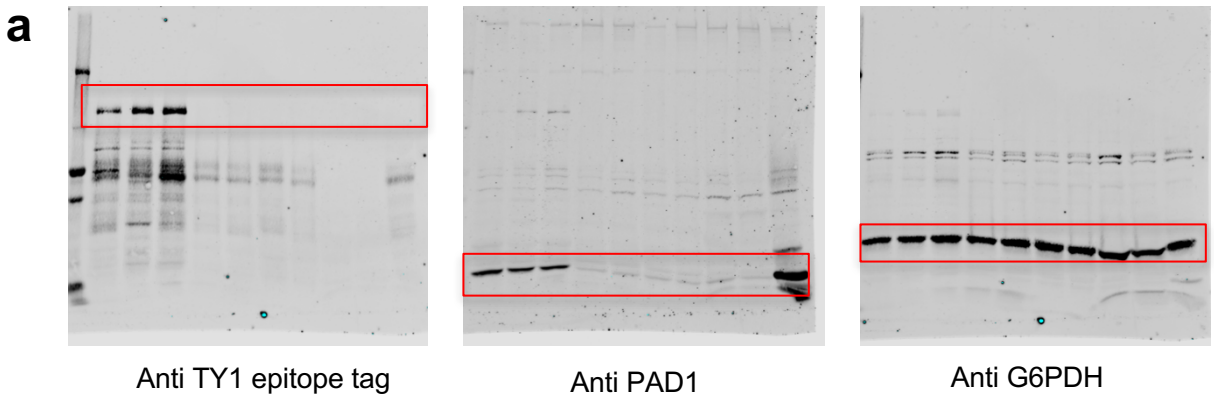

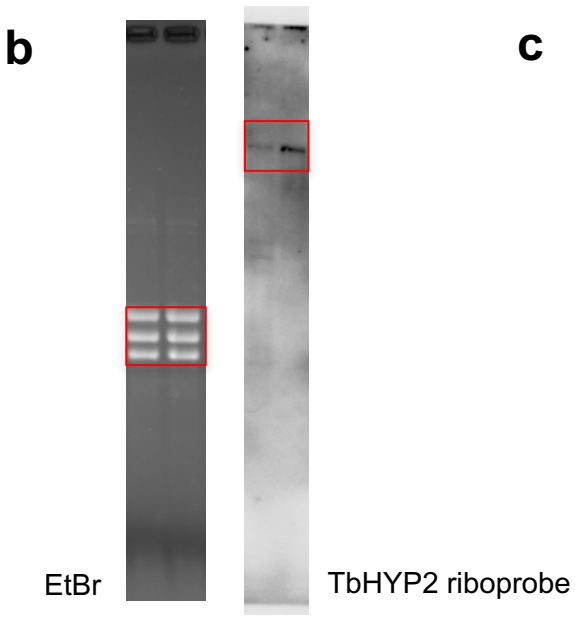

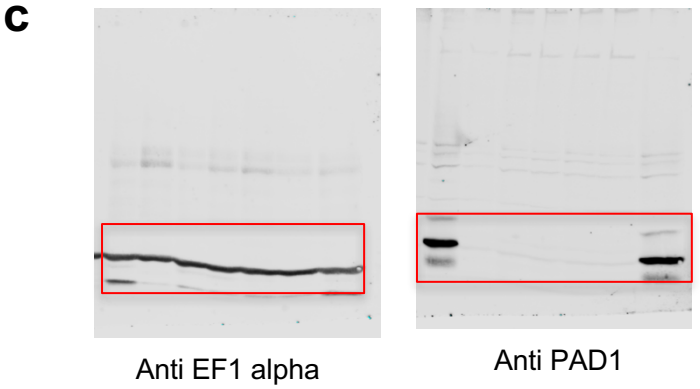

Supplementary Figure 12

Full length gels and blots from the Figures presented in this paper.

a. Figure 2c blots
b. Figure 4d blots
c. Supplementary Figure 4b blots